Journal Pre-proof

Cation-exchange properties of the Mesozoic sedimentary sequence of Northern Switzerland and modelling of the Opalinus Clay porewater

Maria Marques Fernandes, Martin Mazurek, Paul Wersin, Raphael Wüst, Bart Baeyens

PII: S0883-2927(23)00297-4

DOI: https://doi.org/10.1016/j.apgeochem.2023.105852

Reference: AG 105852

To appear in: *Applied Geochemistry*

Received Date: 9 March 2023

Revised Date: 14 November 2023

Accepted Date: 14 November 2023

Please cite this article as: Marques Fernandes, M., Mazurek, M., Wersin, P., Wüst, R., Baeyens, B., Cation-exchange properties of the Mesozoic sedimentary sequence of Northern Switzerland and modelling of the Opalinus Clay porewater, *Applied Geochemistry* (2023), doi: https://doi.org/10.1016/j.apgeochem.2023.105852.

Cation-exchange properties of the Mesozoic sedimentary sequence of northern Switzerland and modelling of the Opalinus Clay porewater

Maria Marques Fernandes[1*], Martin Mazurek[2], Paul Wersin[2], Raphael Wüst[3,4], Bart Baeyens[1]

[1]Paul Scherrer Institut (PSI), Laboratory for Waste Management, 5232 Villigen PSI, Switzerland

[2]Rock-Water Interaction (RWI), Institute of Geological Sciences, University of Bern, Switzerland

[3]National Cooperative for the Disposal of Radioactive Waste (Nagra), CH-5430 Wettingen, Switzerland

[4]Earth and Environmental Science, James Cook University, 4811 Townsville, Australia

Highlights:

- Large dataset of CEC and cation occupancies from the Mesozoic of Switzerland
- Good correlation between CEC and clay mineralogy identified.
- Ni-CEC ≤ Cs-CEC ≤ ΣCATIONS, with differences between them ≤ 20 %.
- Cation occupancies similar for various lithologies with clay content > 20 wt.%.
- Modelled porewaters agree well with data obtained from independent experiments.

* E-mail of corresponding author: maria.marques@psi.ch

Abstract

In Switzerland, radioactive waste management requires the safe disposal of nuclear waste within a deep geological argillaceous sequence that includes the Jurassic-age Opalinus Clay. The process of selecting a suitable site for the disposal is ongoing and involves a rigorous site selection process. As part of this process, site-specific physico-chemical data were collected, which include parameters such as cation exchange capacities (CEC) and exchangeable cation occupancies, in addition to other geochemical and mineralogical data. The mineralogy, CEC and exchangeable cation occupancies of rock samples collected from the various lithologies of cores from seven boreholes across the study areas, namely Zürich Nordost (ZNO), Nördlich Lägern (NL) and Jura Ost (JO) were investigated. Four different CEC methods were applied, and the results obtained are in good agreement. The general trend in the CEC data follows: Cs-CEC ≥ (ΣCATIONS) > Ni-CEC. The higher Cs-CEC values are due to the higher interlayer extraction yields of low hydration cations K^+ and NH_4^+ in illite rich rock samples by the highly selective Cs^+. A clear correlation between the 2:1 phyllosilicate content and the CEC values is observed over the entire sequence, so clay minerals primarily govern cation exchange processes and thus the retention of cations. Finally, for the Opalinus Clay of each of the three study areas, porewater chemistries were modelled based on a combination of mineralogical and physico-chemical data. The calculated porewater compositions are in good agreement with the compositions obtained from squeezing and advective displacement experiments in the laboratory.

Key words:

Exchangeable cations, sedimentary rocks, clay mineralogy, geochemical modelling

1. Introduction

In northern Switzerland, the Jurassic-age Opalinus Clay is an argillaceous sedimentary rock formation that has been identified as the suitable host rock for the deep geological disposal of radioactive waste in Switzerland, among others due to its thickness of >100 m. In Stage 3 of the Sectoral Plan (Sachplan Geologisches Tiefenlager, SGT-E3), Nagra (Swiss National Cooperative for the Disposal of Radioactive Waste) is thoroughly investigating three areas, namely Zürich Nordost (ZNO), Nördlich Lägern (NL) and Jura Ost (JO). The geographic and geological settings as well as profiles of all boreholes are documented in Mazurek et al. (2023). In addition to 3D seismic measurements and drillings into the Quaternary cover, deep borehole investigations aimed to complement and extend previous investigations of the underground geological environment in these areas. The outcome of these investigations and the safety-based comparison of the study areas will contribute to the selection of Nagra's best suited site for a deep geological repository.

Site-specific physico-chemical rock data such as cation exchange capacity (CEC) and exchangeable cation occupancy are, amongst other geochemical and mineralogical parameters, part of the deep borehole investigations and are required for each potential region for the site selection procedure. This study focuses mainly on CEC of rock samples and on the exchangeable cation occupancies of the major alkaline and alkaline-earth elements. CEC is an important rock parameter since it is a measure of the rocks ability to retain cations, and hence, is of key importance for the transport of radionuclides in deep underground argillaceous formations. The CEC predominantly quantifies the permanent negative charge of the rock samples, primarily due to the presence of 2:1 phyllosilicates (Christidis et al., 2023). Cations adsorb onto the planar sites of these minerals through electrostatic bonding. Additionally, CEC can be defined as the sum of exchangeable cations that are present at the clay mineral surfaces of the rock samples. The CEC is directly related to the type and quantity of clay minerals that are present in the rock samples, and consequently, to their ability to adsorb radionuclides.

The in-situ fractional occupancy of exchangeable cations acts as a "fingerprint" for the *in situ* porewater composition of argillaceous rock formations. Typically, the porewater of sedimentary

rock consists primarily of non-reactive solutes such as Cl resulting from the hydrogeological evolution of the rock, and of reactive solutes resulting from equilibrium with the mineral constituents. In argillaceous rocks, the concentrations of dissolved cations are predominantly controlled by equilibrium with cations adsorbed on at clay mineral surfaces and the equilibrium with carbonate and sulphide/sulphate minerals. Hence, the data also provided an opportunity to investigate the composition of the interstitial porewater in the Opalinus Clay. For that, a geochemical model was used to calculate concentrations of major cations and anions. The results were compared with the concentrations obtained from squeezing (SQ) and advective displacement (AD) experiments conducted on the rock samples (Kiczka et al., 2023). This comparison provided valuable information on the accuracy and reliability of the geochemical model in predicting the porewater composition of the Opalinus Clay, and hence, the behaviour of radionuclides in the formation.

2. Materials and Methods

2.1. Origin of the core samples and sample preparation

The rock samples analysed in this study originate from the three study areas (i) Zürich Nordost (ZNO), (ii) Nördlich Lägern (NL) and (iii) Jura Ost (JO), specifically from the cores recovered from the deep boreholes Trüllikon-1-1 (TRU1-1) and Marthalen-1-1 (MAR1-1) from ZNO, Bülach-1-1 (BUL1-1), Stadel-2-1 (STA2-1) and Stadel-3-1 (STA3-1) from NL and Bözberg-1-1 (BOZ1-1) and Bözberg-2-1 (BOZ2-2) from JO (see Mazurek et al., 2023 for localisation of the boreholes and for geological context). In total, 184 rock samples have been investigated in this study by two institutes, namely Paul Scherrer Institut (PSI) and the Rock-Water Interaction (RWI) group at the Institute of Geological Sciences at the University of Bern. An overview of the number of samples and their origin is given in Table 1. The detailed descriptions (lithological type, depth, geological formation, mineralogical composition) of the rock samples are given in the Supporting Information (SI).

Table 1: Number and origin of rock samples analysed by PSI and RWI.

Area	**ZNO**			**NL**		**JO**	
Borehole	MAR1-1	TRU1-1	STA2-1	STA3-1	BUL1-1	BOZ1-1	BOZ2-1
PSI	20	11	20	22	26	32	10
RWI	7	4	3	3	18	5	3

The PSI samples (2 × 3 cm^3 cubes) were vacuum packed after preparation at the Institute of Geological Sciences. Once at PSI, they were transferred into a N_2 flooded glove box (O_2 < 1 ppm) for crushing and storage. The entire sample handling was done inside the glove box. The samples were first crushed by hand in an agate mortar to pieces < 1 cm^3 and then ground in a Retsch mortar grinder to a size < 1 mm. The grinder was cleaned after each sample to avoid cross-contamination. Samples were stored in the glove box in closed, well-labelled containers.

The RWI samples were prepared by removal of rims and disintegration to a few mm^3. About 30 g of the rock was then immediately immersed in 30 ml of degassed and N_2-purged Ni-en solutions in polypropylene tubes, then quickly transferred to an anaerobic glovebox (95:5 N_2:H_2 atmosphere equipped with two Pd catalysts) and reacted for 24 h. After extraction, phase separation was conducted by centrifugation and filtration (0.2 μm PES filters) and stored for analyses.

2.2. Mineralogical analyses

Details of the sample preparation and analysis are described in Mazurek and Aschwanden (2020). Representative sample material was crushed and then ground using a Retsch McCrone XRD-mill, leading to a unimodal grain-size distribution with a median <5 μm, which is suitable for powder X-ray diffraction analysis. Non-oriented X-ray patterns were collected with a PANalytical CubiX^3 diffractometer using a Cu source. The data was analysed using the PANalytical HighScore Plus v. 4.x software together with a lab-internal database and then quantitatively evaluated based on structural data and using the Rietveld method (Rietveld, 1969), or, when clay minerals present, using a combined Rietveld and Pawley approach (Pawley, 1981), optionally cross-checked with Coelho Software TOPAS-Academic v. 6. Corundum (20 wt.%) was added as an internal standard. Carbonate mineral contents were calibrated via chemical analysis of TIC using a CNS analyser, and pyrite contents were obtained from the determination of S, except in anhydrite-bearing samples. For the structural identification of the clay minerals,

which are characterised by two-dimensional sheets and the order of the tetrahedral and octahedral sheets, the chemical variability and structural disorder do not allow routine quantification by the Rietveld method. The identification and the quantification of clay mineral phases was based on the determination of their relative proportions using oriented powder X-ray diffraction patterns (dry, glycolated, heated). For the quantification of the relative proportions of clay minerals, a full pattern fit method analogous to the ARQUANT approach (Blanc et al., 2007) was developed. Absolute contents were calculated by difference (100 % minus sum of all non-clay minerals). Clay minerals include illite, illite/smectite mixed layers, kaolinite, chlorite and chlorite/smectite mixed layers and are expressed as end-members of illite, smectite, kaolinite, chlorite in this study. Thus, for example, the smectite component from illite/smectite mixed layers is attributed to the smectite end-member, and the illite component accordingly to the illite end-member.

2.3. Cation exchange determination

2.3.1. Ni-CEC and Σ CATIONS

The CEC of the rock samples and the exchangeable cations Na, K, Mg, Ca and Sr were determined using the highly selective Ni-triethylenediamine (Ni-en) complex (Peigneur, 1976). The Ni-en data presented in this study are denoted as Ni-CEC. Excess Ni-en allows to displace the cations from the exchange sites and to saturate them. In addition, the CEC was also estimated from the sum of total released cations after correction for the dissolved anions (Σ CATIONS), as described in Section 2.4. PSI only determined Ni-CEC whereas RWI estimated in addition the exchangeable cation compositions.

PSI samples: The CEC of the rock samples was determined by using the Ni-en complex radiolabelled with ^{63}Ni. A Ni-en excess of already 20 % of the CEC of the sample is sufficient to saturate the exchange complex (Bradbury and Baeyens, 1998). The Ni-CEC measurements were carried out under ambient air conditions. The procedure consists essentially of an adsorption experiment with ^{63}Ni labelled Ni-en. The Ni-en solution was prepared by the addition of uncharged ethylenediamine to a $Ni(NO_3)_2$ solution to obtain a stable Ni-triethylenediamine complex at a total concentration of 3.3 mM. 30 ml of the ^{63}Ni-en solution were added to ~ 1 g of

158 rock sample, pre-weighed into polypropylene centrifuge tubes, to give a solid to liquid (S:L) ratio
159 of ~ 32 g·L^{-1}. The tubes were closed, shaken end-over-end for 1 day, centrifuged at 108'000 $g_{(max)}$,
160 and the supernatant solutions were radio-assayed using a Packard Tri-Carb liquid scintillation
161 counter. The pH of the supernatant was measured after phase separation and ranged from 8 to 9.

162 The Ni-en adsorbed (Ni-en$_{ads}$) in meq/kg (equal to the CEC) was calculated from the
163 redistribution of the radiotracer between the solid and liquid phases and was calculated from:

164 $$\text{Ni-en}_{ads} = \frac{A_{in}\text{-}A_{out}}{A_{in}} \cdot \text{Ni-en}_{in}$$

165 where A_{in} = initial ^{63}Ni activity (cpm); A_{out} = final ^{63}Ni activity (cpm) and Ni-en$_{in}$ = initial
166 amount of Ni-en (in meq/kg). The average results of triplicate, respectively duplicate, experiments
167 for the three regions are summarized in the tables in the appendix.

168 ***RWI samples:*** Ni-CEC determinations were also carried out by RWI by using the Ni-en
169 complex as described above, however at much higher S:L ratios (~ 1 kg/L with 30 g of solid and
170 30 g of Ni-en solution) and only with stable Ni. The initial Ni-en concentrations were set to
171 correspond to double amount of the expected CEC and were usually close 100 mmol/L. The
172 amount Ni exchanged was quantified by ICP-OES analysis. In the RWI samples, the released
173 cations and anions were determined in the Ni-en extraction (Ni-ex) experiments. After filtration,
174 the supernatant solutions were analyzed for cations (Na, Ca, Mg, K, Sr, Ba, Fe) and anions (Cl,
175 SO_4, F, Br, NO_3) by ion chromatography. The concentrations of Fe, Ba and Br turned out to be
176 close to or below detection. NO_3 concentrations were high because nitrate is part of the Ni-en
177 stock solution. NH_4 was not analyzed in these extraction experiments. The analyses of total cation
178 and anion concentrations allow to determine the ΣCATIONS in the Ni-ex experiments (Section
179 2.4).

180 *2.3.2. Cs-CEC and ΣCATIONS*

181 Similar to the Ni-CEC method, the addition of the highly selective Cs cation to rock samples
182 can saturate the exchange complex, if the added Cs is in excess to the CEC. The consumption of
183 Cs equals the CEC of the samples and is denoted as Cs-CEC in this paper. The determination of
184 the CEC with Cs requires a higher excess of Cs compared to Ni-en. In this study we have used a

fivefold Cs excess, optimized based on the Ni-en CEC results which were carried out and evaluated prior to the Cs-CEC measurements. The major cations Na, K, Mg and Ca and two minor cations NH_4 and Sr are displaced from the cation exchange sites of the rock samples by using the highly selective Cs cation. Similar to the Ni-ex experiments the Cs extraction (Cs-ex) experiments allow to determine the CEC of the rock samples by calculating the sum of total released cations after correction for the dissolved anions (ΣCATIONS). The correction method is described in detail in Section 2.4. The Cs method was only applied to the PSI samples.

The experiments were performed in closed tubes in a N_2 flooded glove box (O_2 < 1 ppm) to avoid oxidation of the samples and the equilibration with CO_2. The exchangeable cations were displaced by using a fivefold equivalent excess of Cs with respect to Ni-CEC of the samples, determined prior by the Ni-en method (see section 2.3.1). The 5-fold Cs excess was quantified by optimising the S:L ratio in the Cs extraction (Cs-ex) experiments (*i.e.*, by adapting the mass of rock samples). The initial CsCl concentration in the Cs-ex experiments was 33 mM. Each experiment was set up in duplicate. The tubes with the rock samples and the appropriate CsCl solution were shaken end-over-end for 1 day, centrifuged at 108'000 g (max), and the supernatant solutions were analysed for the cations Na, K, NH_4, Mg, Ca and Sr and the anions SO_4 and total inorganic carbon (TIC). The pH of the supernatants was measured after phase separation.

The amount of dissolved Cl^- was determined in separate aqueous extraction (H_2O-ex) experiments by equilibrating 1 g of rock sample with 30 ml de-ionised water (S:L ratio of ~30 g/L). Phase separation was as described above and the supernatant was analysed for Cl^-. The reason for these additional H_2O-ex experiments was because the use of CsCl (33 mM) as extract solution in the Cs-ex experiments did not allow to determine the Cl inventories of the rock samples reliably.

The concentrations of Na, K, Mg, Ca, Sr, S and Cs were determined by inductively coupled plasma optical emission spectrometry (ICP-OES). Cl, NH_4 and SO_4 were quantified by ion chromatography (IC). The TIC analysis was carried out by a Dohrmann Carbon Analyser. The concentrations of extracted (exchangeable and dissolved) cations and of dissolved anions are summarized in the SI.

2.3.3. CEC calculated from the clay mineralogy: Clay-CEC$_{calc}$

The CEC of rock samples results from different clay mineral contents and the magnitude of their respective CEC values. Hence, the CEC of rock samples can be calculated from the mineralogical composition of the samples (bulk clay content and detailed composition of the clay fraction) by using the CEC values of the pure clay minerals present in the samples scaled to their weight percentages in the samples, which is referred to as Clay-CEC$_{calc}$. The Clay-CEC$_{calc}$ values of the rock samples where the bulk and clay mineralogy data is available are included in the SI. The composition of the clay mineral fraction is expressed as end-member compositions (i.e., illite, kaolinite, chlorite, and smectite; see Section 2.2) and is used to calculate the Clay-CEC$_{calc}$.

The CEC values used for the pure clay minerals in this study were taken from the literature: 870 meq/kg for smectite (Bradbury and Baeyens, 1995), 225 meq/kg for illite (Baeyens and Bradbury, 2004), 28 meq/kg for kaolinite (Allard et al., 1983), and 50 meq/kg for chlorite (Allard et al., 1983). It should be noted that the CEC values for pure clay minerals are not fixed but rather subject to variations depending on the selected source. Note that the dominant clay mineral does not necessarily determine the magnitude of the CEC of the rock sample. For example, the CEC of kaolinite is ~10 times lower than that of illite.

2.4. Determination of exchangeable cations: correction method

The cations extracted in the Ni-ex and Cs-ex experiments do not only arise from the cation exchange sites of the clay minerals in the rock samples, but also from the dissolution of minerals and of salts precipitated from the porewater during drying. To accurately estimate the concentrations of displaced cations solely originating from the cation exchange sites, the total extracted cations must be corrected with the associated dissolved anions (Bradbury and Baeyens, 1998; Hadi et al., 2019). As mentioned before, chloride was not measured in the Cs-ex experiments but in separate H_2O-ex experiments.

The corrections were based on detailed mineralogical data and the soluble salt content of the samples. Although the total amount of exchangeable cations (expressed in meq/kg) should correspond ideally to the CEC of the rock sample, this is not always the case for complex rock systems. This is because all exchangeable cations may not be well identified and/or recovered in

241 the extracting solution. If the sum of the total extracted cations is very close to the sum of the total
242 extracted anions (both expressed in an equivalent scale), which is the case for rock samples with
243 very low clay mineral contents and very low CEC, no reliable analysis on exchangeable cation
244 loadings can be made.

245 An overview of the mineralogical composition across the various formations and rock types is
246 described by Mazurek et al. (2023). In the present study a range of different rock samples, ranging
247 from claystones to marls to almost pure limestones, plus some anhydrite-bearing samples have
248 been analysed. The mineralogical data for each individual sample are given in the SI.

249 For all the rock samples investigated by PSI and RWI, total extracted Na concentrations were
250 corrected for total dissolved Cl concentrations since it is assumed that Cl originates from the
251 dissolution of NaCl. The total extracted concentrations of K, NH_4, Mg and Sr were not corrected
252 in either the PSI or RWI samples.

253 The total extracted Ca concentrations were corrected for total dissolved TIC in the Cs-ex
254 experiments. Since the intrusion of CO_2 was avoided during the experiments and degassed
255 solutions were used, the dissolution of calcite generates equal molar amounts of Ca^{2+} and CO_3^{2-}.
256 If the concentrations of dissolved Fe and the exact content of dolomite/ankerite were available, it
257 would have been possible to distribute the amount of dissolved TIC more accurately among Ca,
258 Fe and Mg. Although this study's approximation may lead to a slight underestimation of the Ca
259 occupancies in favour of Mg (and very few cases of Sr where extracted concentrations were
260 generally very low), it does not affect the sum of exchangeable cations. In the case of RWI data,
261 TIC was not included in the correction procedure, because its concentrations were very low (well
262 below 1 mM) in the Ni-en extracts at the high S/L ratios applied (Wersin et al., 2022).

263 Total extracted dissolved SO_4 was corrected with total extracted Ca in both the Cs-ex and Ni-
264 ex experiments. As discussed by Bradbury and Baeyens (1998), SO_4 could also be corrected with
265 Na which leads to different Na and Ca loadings. However, squeezing results indicate that the
266 correction of Ca with SO_4 is more realistic (Kiczka et al., 2023; Wersin et al., 2023).

267 Finally, the exchangeable occupancies of Na, K, NH_4, Mg, Ca and Sr of the rock samples
268 (expressed in an equivalent scale) were calculated from the extracted cation concentrations after

correction with the dissolved anionic species, as described above, and then normalized to the dry weight of the rock samples. The equivalent fraction of each exchangeable cation (N_B = $N_{Na,}$ $N_{K,}$ $N_{NH4,}$ $N_{Mg,}$ $N_{Ca,}$ N_{Sr}) or group of cations (N_B = $N_{K+NH4,}$ $N_{Mg+Ca+Sr}$) was obtained by dividing the sum of each exchangeable cation or group of cations (in meq/kg) by the sum of all exchangeable cations (ΣCATIONS) (in meq/kg). For the PSI samples ΣCATIONS was obtained from the Cs-ex experiments whereas for the RWI samples ΣCATIONS was obtained from the Ni-ex experiments.

2.5. Geochemical modelling

A geochemical model can be applied to the physico-chemical parameters, the mineralogical data and some additional parameters to estimate the composition of the in-situ porewater of the Opalinus Clay in the different study areas. The modelling follows the method proposed by Bradbury and Baeyens (1998) and uses the mineral equilibrium calculations of the PSI/Nagra thermodynamic database compiled by Thoenen et al. (2014). The Davies approach was used for the calculation of the solution activity coefficients (Davies, 1962). Cation exchange equilibria between Na and K, NH_4, Mg, Ca and Sr were calculated using the Gaines and Thomas convention (Gaines and Thomas, 1953). The selectivity coefficients (K_c) for the Na-K, Na-Mg, Na-Ca and Na-Sr equilibria were taken from Wersin et al. (2022) and are consistent with the values used by Kiczka et al. (2023). The K_c value for Na-NH_4 exchange was taken the same as for the Na-K exchange since K and NH_4 have similar exchange behaviour on 2:1 clay minerals (De Preter, 1990). The geochemical equilibrium calculations were performed with the MINSORB code which is based on MINEQL (Westall et al., 1976) modified to include cation exchange (Bradbury and Baeyens, 1998).

3. Results and discussion

3.1. Mineralogy and cation exchange capacity

3.1.1. Mineralogical analyses

The most abundant minerals in the samples are quartz, calcite and various clay minerals. Clay minerals identified include illite, illite-rich illite/smectite mixed layers, kaolinite, chlorite and minor chlorite-smectite mixed layers (details in Mazurek et al. (2023)). The clay mineral contents reported here are based on end-member compositions, *i.e.*, the proportions of illite, smectite and

297 chlorite in mixed-layer phases are attributed to the respective pure phases (see Section 2.2). The
298 illite end-member and kaolinite dominate by quantity (Fig. 1), even though the relative
299 proportions vary markedly between formations (see Mazurek et al. (2023)).

300 Fig. 1 displays mineral content profiles for JO, NL and ZNO. Clay minerals (sub-divided and
301 plotted as end-members illite, smectite, kaolinite, chlorite), calcite and quartz are the predominant
302 mineral phases, accounting for more than 80 wt.% of the rock composition. Minor minerals, such
303 as dolomite/ankerite, siderite, K-feldspar, plagioclase and pyrite, are present at few percentages
304 only. Anhydrite is only present in the Keuper below the Klettgau Formation. For a comprehensive
305 representation of mineralogical compositions, including all samples studied in the whole
306 programme, refer to Mazurek et al. (2023).

307 *3.1.2. CEC results*

308 CEC measurements have been determined on 141 (PSI) and 43 (RWI) rock samples according
309 to the methods described in detail in Section 2.3. Four different methods have been applied. The
310 Ni-CEC and Cs-CEC are direct measurements whereas ΣCATIONS and Clay-CEC_{calc} are indirect
311 methods. Fig. 1 illustrates the results of the four different methods for the PSI samples (coloured
312 symbols) and RWI samples (black symbols) for the three study areas.

313

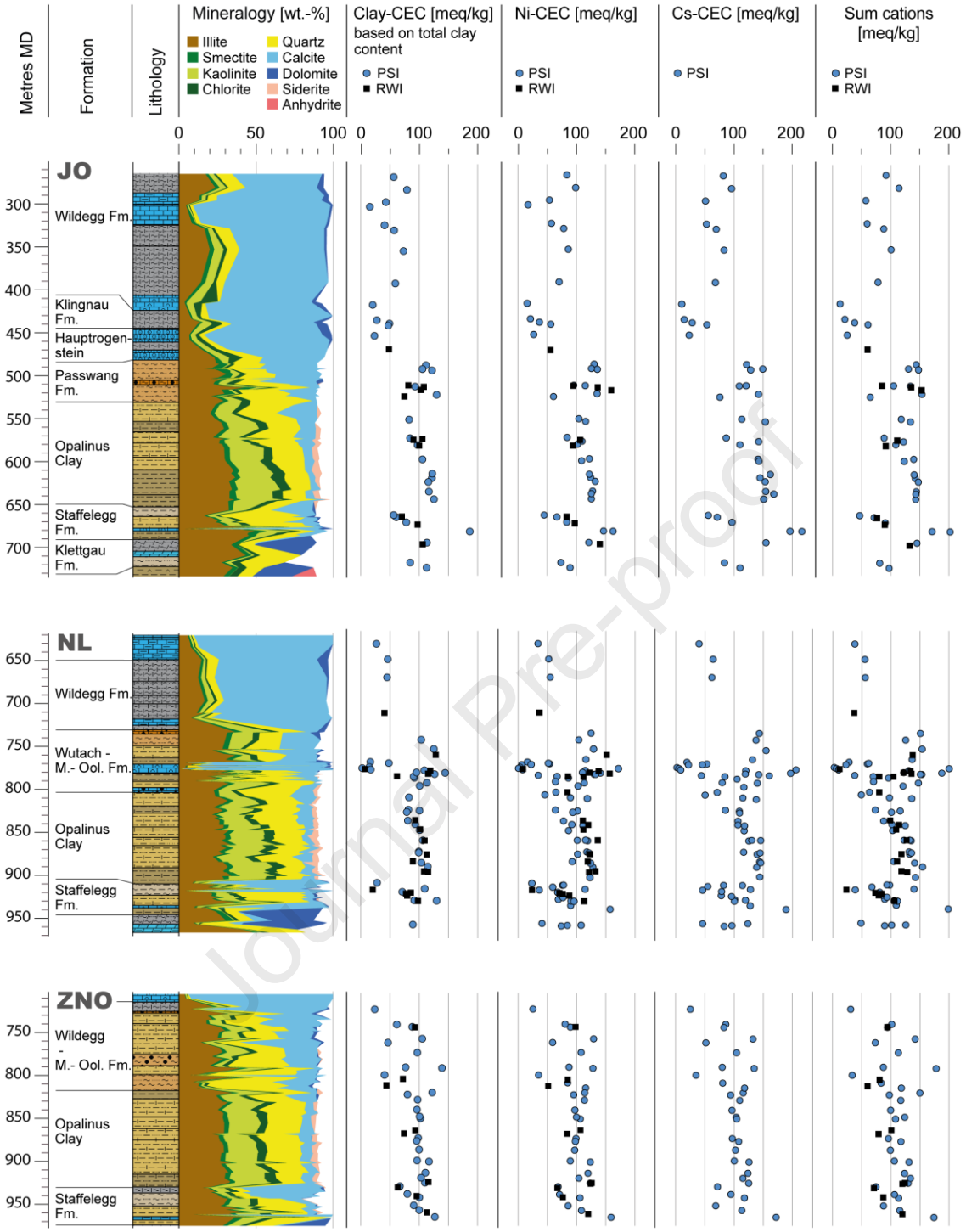

Fig. 1. Profiles of the study areas (JO, NL, ZNO) showing representative stratigraphic sections and the mineralogical data. The formation depths are adjusted to the profiles of BOZ1-1 (JO), STA2-1 (NL) and TRU1-1 (ZNO). Clay minerals, quartz and calcite dominate the composition of these Mesozoic rocks. The cation data includes results from Clay-CEC_{calc}, Ni-CEC, Cs-CEC and ΣCATIONS methods.

A general observation is that there is no offset between PSI and RWI samples suggesting good agreement although the measurements were not carried on identical samples. Fig. 1 provides an

initial overview of the variation in CEC values along the depth profile and their correlation with the content of clay minerals. It also illustrates the variability in CEC values across different lithological units.

Table 2 presents a summary of the CEC data, displaying the numerical values obtained from the four different methods used for each of the three study areas. The results are divided into four main units: (i) Malm, (ii) Dogger above Opalinus Clay, (iii) Opalinus Clay, and (iv) Staffelegg Formation. The number of samples analysed for each unit is shown in italics next to the unit names. The values in Table 2 represent the average CEC values with the corresponding standard deviations given in parenthesis. The statistical analyses include samples that were analysed either at PSI or RWI except for Cs-CEC (only PSI).

Table 2: Summary of CEC measurements by 4 different methods on the main units of the 3 study areas. D.A.O. = Dogger above Opalinus Clay.

Area	**Units**	**Clay-CEC$_{calc}$**	**Ni-CEC**	**Cs-CEC**	**ΣCATIONS**
		[meq/kg]			
ZNO	Malm [1]*	24.0	24.9	25.9	31.1
	D.A.O. [13]	78.9 (29.8)	88.7 (28.6)	91.5 (32.7)	94.4 (38.2)
	Opalinus Clay [17]	101.3 (12.2)	106.9 (13.0)	109.8 (10.8)	112.7 (18.3)
	Staffelegg Fm. [9]	93.5 (20.6)	95.9 (30.9)	107.5 (38.2)	102.7 (33.4)
NL	Malm [5]	40.1 (7.6)	43.8 (10.7)	54.5 (13.3)	44.6 (12.4)
	D.A.O. [31]	80.5 (45.6)	85.7 (52.5)	96.5 (62.1)	96.2 (56.4)
	Opalinus Clay [30]	99.0 (11.5)	104.3 (22.0)	118.3 (25.9)	109.3 (25.1)
	Staffelegg Fm. [19]	73.5 (36.3)	77.2 (31.5)	100.1 (37.0)	90.3 (38.2)
JO	Malm [8]	53.3 (20.0)	68.9 (25.5)	72.1 (16.4)	84.9 (21.0)
	D.A.O. [15]	76.2 (38.8)	87.9 (50.1)	81.8 (53.3)	92.0 (53.0)
	Opalinus Clay [15]	105.7 (14.8)	114.6 (13.9)	140.0 (23.3)	126.6 (20.2)
	Staffelegg Fm. [7]	91.8 (46.6)	98.6 (42.6)	127.8 (74.2)	106.4 /57.8)

*[x]: number of samples from the given unit

The data compilation in Table 2 reveals several clear trends. Firstly, the CEC values for all units in the three study areas follow a general sequence: Clay-CEC$_{calc}$ ≤ Ni-CEC ≤ Cs-CEC ≤ ΣCATIONS, with differences between them being ≤ 20 %. The reason for the discrepancy between *e.g.*, Cs-CEC and ΣCATIONS is further elaborated in Section 3.1.4. Secondly, the CEC values for the Malm samples are significantly lower compared to those from the other units with comparable CEC values although with a higher variability. Thirdly, the CEC data for Malm, Dogger above Opalinus Clay and Staffelegg Formation exhibit much larger standard deviations compared to the

samples from the Opalinus Clay, highlighting the more heterogeneous rock composition of these units.

3.1.3. Correlation of Ni-CEC with total clay content and Clay-CEC$_{calc}$

The CEC of rock samples can be attributed to clay minerals, as they possess a permanent negative charge at the planar sites of their surface structures, which are responsible for the cation exchange properties. Fig. 2a shows the relationship between Ni-CEC values and clay mineral content in the bulk rock samples for 141 PSI (blue symbols) and 43 RWI (brown symbols) samples, indicating a fair correlation. Fig. 2b shows the correlation between Ni-CEC and Clay-CEC$_{calc}$ calculated from the detailed clay mineralogy as described in Section 2.3.3. This correlation is markedly better because it takes into account the relative proportions of the individual clay minerals, which vary markedly over the studied profiles (Mazurek et al. 2023). Illite and kaolinite are the two dominant clay minerals in most of the rock samples as illustrated in Fig. 1. The number of samples in Fig. 2b is lower than in Fig. 2a since detailed clay mineralogy was not always available for all the samples. In all cases, the clay mineralogy was determined on sample material not identical (but adjacent) to the material on which the Ni-CEC was measured, and yet the correlation method relies on the transferability of the clay composition to the CEC measurements of each sample.

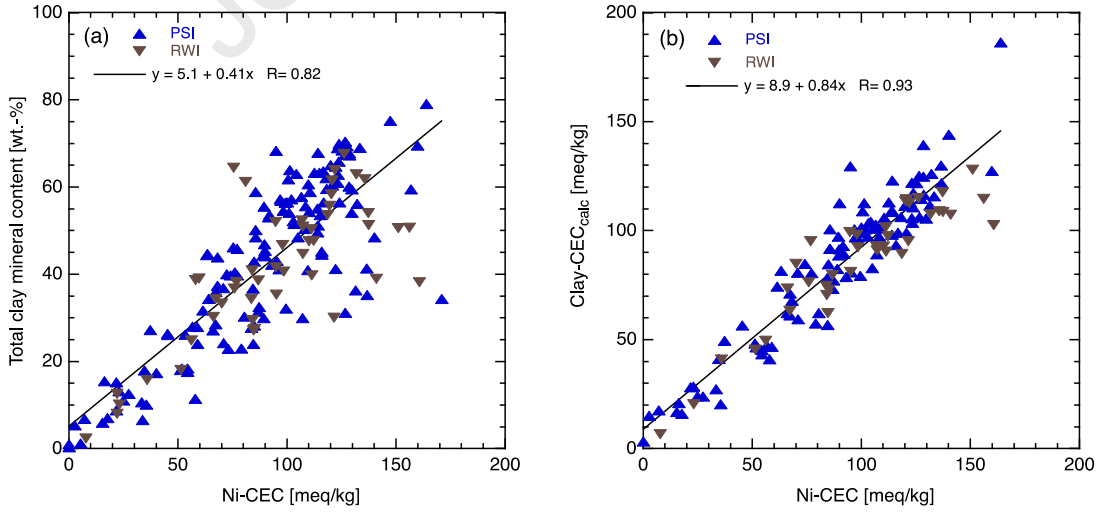

Fig. 2. Correlation of Ni-CEC with (a) total clay mineral content and (b) Clay-CEC$_{calc}$ for all rock samples from ZNO, NL and JO.

3.1.4. Correlation of Ni-CEC with Cs-CEC and ΣCATIONS

The use of highly selective Cs^+ or Ni-en^{2+} in concentrations high enough to saturate the cation exchange sites in the sample allows to determine the CEC by measuring the consumption of the index cation (Cs or Ni-en). Fig. 3a shows the Ni-CEC and Cs-CEC results and a strong correlation exists between the two different methods, whereas the Cs-CEC method consistently yields higher CEC values compared to the Ni-CEC method, as indicated by the slope of 1.2. This is attributed to the higher selective displacement of K and NH_4 from illite by Cs in contrast to Ni-en.

The methods of Cs and Ni-en extraction enable the determination of the CEC of the rock samples by quantifying the displaced cations from the exchangeable sites. The quantification of dissolved salts and minerals is accomplished by detecting the anions present in the Cs-ex and Ni-ex experiments. The determination of CEC (denoted as ΣCATIONS or as SUM CATIONS in the figures) is obtained from the sum of the corrected cations (total extracted cations minus dissolved anions). Fig. 3b shows the correlation between Ni-CEC and ΣCATIONS obtained from Cs-ex (PSI) and from Ni-ex (RWI) experiments. The results obtained from both methods exhibit strong correlations, thereby enhancing the credibility and confidence in the applicability and reliability of these methods for determining cation occupancies. Nonetheless, ΣCATIONS derived from Cs-ex experiments yield persistently higher values than the Ni-CEC data (slope = 1.2), whereas ΣCATIONS obtained from the Ni-ex experiments are consistently lower than the Ni-CEC data (slope = 0.87). The reason for the former observation is discussed above whereas the reason for the latter observation is not clear but was also observed by Bradbury and Baeyens (1998) for Ni-en displacement experiments on an Opalinus Clay sample from Mont Terri.

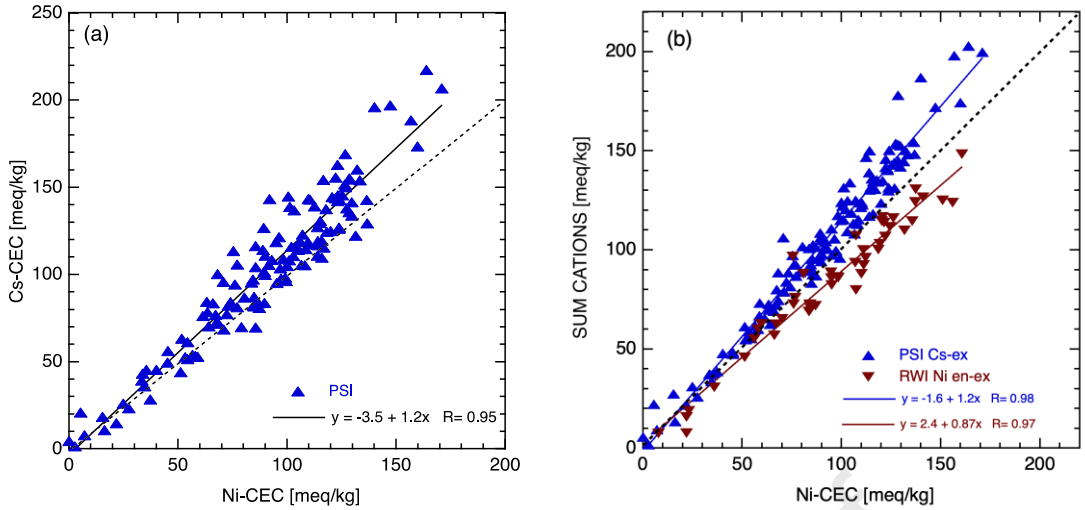

Fig. 3. Correlations of Ni-CEC with: (a) Cs-CEC and (b) ΣCATIONS obtained from Cs displacement experiments (blue symbols) and from Ni-en displacement experiments (brown symbols) for all samples from the three study areas. The dotted lines represent the one-to-one Cs-CEC/ΣCATIONS and Ni-CEC correlation.

3.2. Estimates of in situ cation occupancies

3.2.1. Correction method

The correction method described in Section 2.4 and applied to all the rock samples is illustrated in Fig. 4 where the total extracted anions Cl_{TOT}, SO_{4TOT} and TIC_{TOT} and cations Na_{TOT} and Ca_{TOT} expressed in mmol/kg are plotted together as depth profiles for each study area. As discussed in Section 2.4, Na_{TOT} is corrected with dissolved Cl_{TOT} to obtain the exchangeable Na (Na_{EX}) loading, i.e., $Na_{EX} = Na_{TOT} - Cl_{TOT}$ whereas Ca_{TOT} is corrected with $SO_{4,TOT}$ and TIC_{TOT}, to obtain exchangeable Ca, *i.e.*, $Ca_{EX} = Ca_{TOT} - [SO_{4,TOT} + TIC_{TOT}]$. As mentioned before, the RWI data were not corrected with TIC. The detailed data analyses are given in the SI.

The correction of Na_{TOT} with Cl_{TOT} is small for all samples as illustrated in Fig. 4 (Na-Correction) where Na_{TOT} is compared with corrected Na. Only for 3 limestone samples from the Herrenwis Unit from the NL area this was not the case, and hence, no reliable Na_{EX} data could be derived (see yellow highlighted Na_{EX} values in the SI).

The correction of Ca with the sum of the total dissolved SO_4 and TIC is illustrated in Fig. 4 (Ca-Correction). The SO_4 inventories (~2 mmol/kg) are low in all cases and the correction with total Ca is small. The dissolved TIC is rather large because the Cs extractions were carried out at

406 relatively low S:L ratios (~30 g/L), which led to the dissolution of calcite. The RWI samples were
407 not corrected for TIC because calcite dissolution was suppressed through the common ion effect
408 caused by the high S:L ratio (~1000 g/L) used in the Ni-ex experiments. However, the corrected
409 Ca values are still reliable for deriving the Ca occupancies on exchange sites for most of the rock
410 samples.

411 From the 184 rock samples investigated only 11 samples could not be analysed for obtaining
412 reliable cation occupancies. The samples BUL1-1-845.05 (with 98 wt.% calcite), STA2-1-960.43
413 (with 88 wt.% dolomite) and BOZ1-1-808.61 (with 97 wt.% anhydrite) contain no clay minerals
414 and consequently no CEC or exchangeable cations can be determined. In the samples BOZ1-1-
415 438.20 (61 wt.% carbonates) and BOZ1-1-452.61 (83 wt.% carbonates), the calculated Ca_{EX}
416 values are 2.0 mmol/kg and 0.7 mmol/kg, respectively, and are too low to be reliable. For the
417 remaining 6 samples, namely BOZ1-1-416.35 (76 wt.% carbonates), BOZ1-1-434.29 (78 wt.%
418 carbonates) from the JO area and BUL1-1-815.90 (94 wt.% carbonates), BUL1-1-828.17 (94
419 wt.% carbonates), BUL1-1-840.45 (82 wt.% carbonates) and BUL1-1-851.50 (90 wt.%
420 carbonates) from the NL area, negative Ca_{EX} values are calculated and cannot be treated further.
421 It is noticeable that most of these samples are calcareous and have a low clay mineral content
422 (except BOZ1-1-438.20). In summary, the eleven samples mentioned above were considered
423 unsuitable for inclusion in the calculation of the fractional cation occupancies due to their inability
424 to undergo the Ca-correction method or by the absence of clay minerals. Conversely, for all other
425 samples, the determination of the exchangeable cation loadings on the planar sites of the clay
426 minerals was considered reliable.

427 *3.2.2. Derivation of fractional occupancies (N_B values)*

428 The N_B values are calculated from the exchangeable cation loadings divided by the ΣCATIONS
429 as discussed in detail in Section 2.4. Fig. 4 shows along the profiles of the study areas (JO, NL,
430 ZNO) the N_B values for Na, K, NH_4, Mg, Ca and Sr. The results from the PSI and RWI samples
431 (presented with the same symbols for simplicity) are included in Fig. 4. For almost all samples
432 investigated the following trend in observed: $N_{Na} > N_{Ca} >> N_{Mg} \sim N_K >> N_{NH4} \sim N_{Sr}$ for all study
433 areas. Only in the carbonate-rich Wildegg, Klingnau and Hauptrogenstein formations in JO where

salinity is low N_{Ca} values are higher than N_{Na} values. Noticeable is that this trend is not observed for the carbonate-rich Wildegg formation in NL where N_{Na} values are higher than N_{Ca} values.

The N_{Na}, N_{K+NH4} and $N_{Mg+Ca+Sr}$ values for all samples from the three study areas are summarized in the SI and illustrated in the ternary plot (Fig. 5). In this graphical presentation, K and NH_4 have been grouped since their cation exchange behaviour is very similar ${}^{K}_{NH4}K_c \sim 1$ (De Preter, 1990). The alkaline-earth cations Mg, Ca and Sr are also grouped since the exchange behaviour against Na is taken to be the same in this study (${}^{Mg}_{Na}K_c = {}^{Ca}_{Na}K_c = {}^{Sr}_{Na}K_c = 5$). Fig. 5a illustrates the results of these three parameters for all the PSI and RWI samples from the Opalinus Clay. Clearly, the N_B values for these samples are closely clustered. A notable observation from Fig. 5a is the systematic elevation of N_{K+NH4} values of the PSI samples (represented by closed symbols) relative to the RWI samples (open symbols). The divergence is due to the fact that the highly selective Cs yields higher exchangeable K and that the NH_4 release in the RWI extraction experiments was not accounted for. The lower N_{K+NH4} values are compensated for by higher N_{Na} and/or $N_{Mg+Ca+Sr}$ values since $N_{Na} + N_{K+NH4} + N_{Mg+Ca+Sr} = 1$. Fig. 5b shows the ternary plot for the three groups of exchangeable cations for all remaining samples from the units above and below the Opalinus Clay. The data for these samples show a higher scatter compared to the data presented in Fig. 5a confirming higher heterogeneities in these formations. The data in Fig. 5 show that the Opalinus Clay across all three areas has similar fractional occupancies with a limited range in contrast to the overlying and underlying rock units.

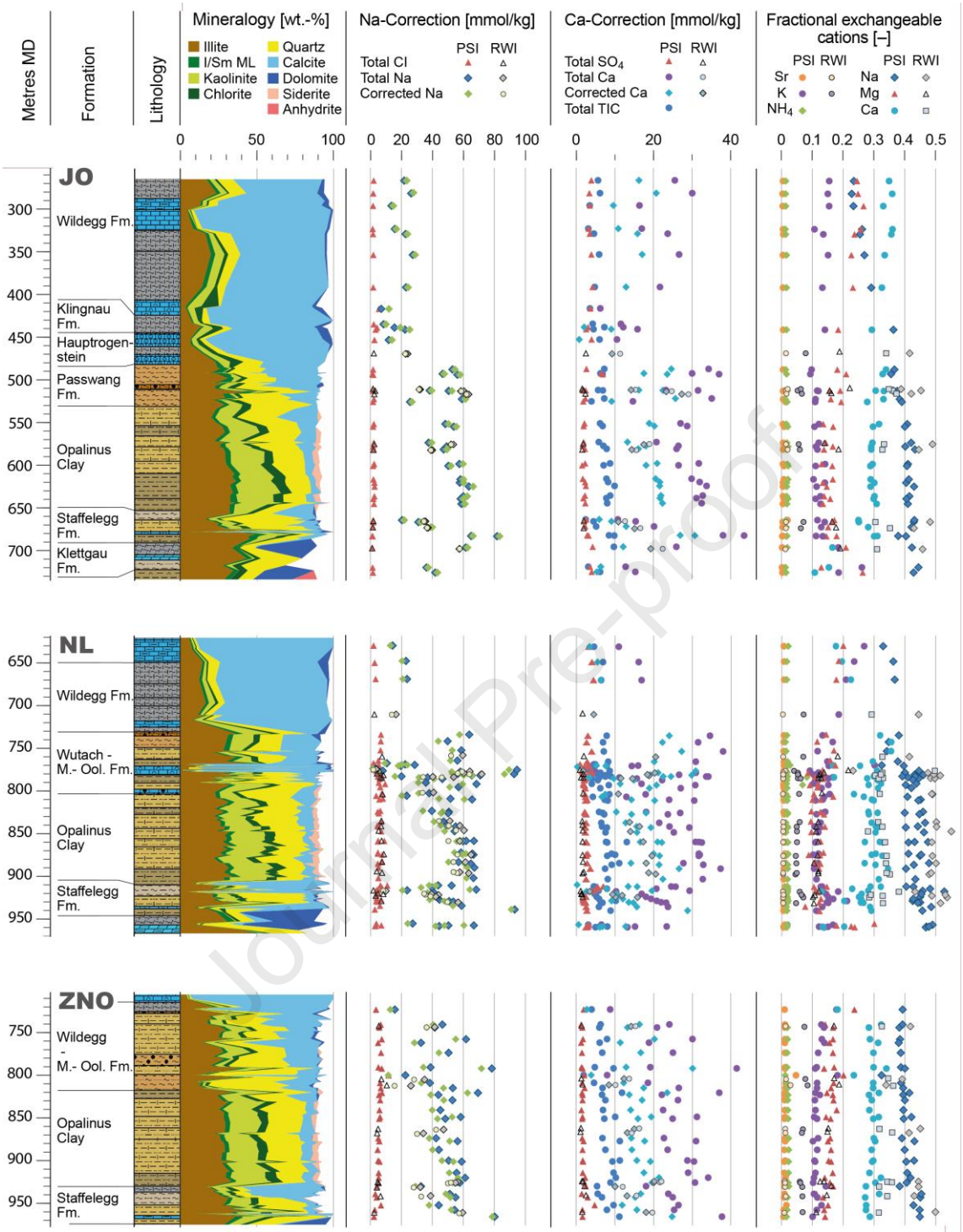

Fig. 4. Profiles of the study areas (JO, NL, ZNO) showing representative stratigraphic sections and the mineralogical data. The formation depths are adjusted to the profiles of BOZ1-1 (JO), STA2-1 (NL) and TRU1-1 (ZNO). The cation data includes results from Na-Correction method, Ca-Correction method and the fractional exchangeable cations Na, K, NH_4, Mg, Ca, and Sr.

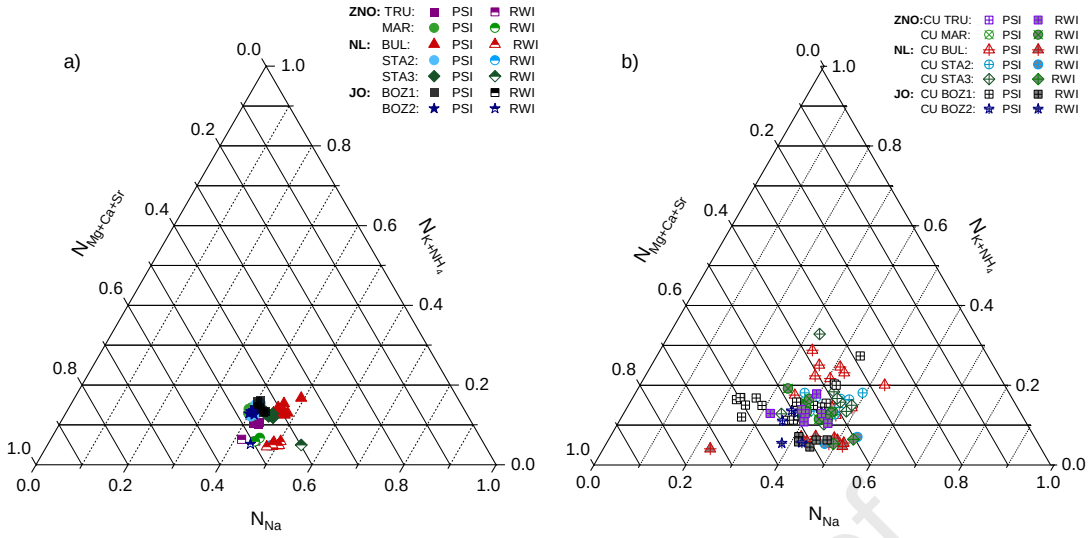

Fig. 5. Ternary representation of N_{Na}, N_{K+NH4} and $N_{Mg+Ca+Sr}$ determined for the samples from (a) Opalinus Clay and (b) the formations above and below the Opalinus Clay for ZNO, NL and JO.

Fig. 6 illustrates the key data for the Jurassic samples in a Füchtbauer triangle (Füchtbauer, 1988) concerning the clay mineralogy and physico-chemical parameters investigated in this study. The data displayed in Fig. 6 are (i) 2:1 clay minerals (illite+smectite+chlorite end-members) in wt.%, (ii) Ni-CEC in meq/kg, (iii) N_{Na}, (iv) N_{K+NH4} and (v) $N_{Mg+Ca+Sr}$. The values presented in Fig. 6 are the average values (with ±standard deviations and the number of samples in parenthesis) for eight lithological rock types shown in the triangle. The 2:1 clay mineral content of argillaceous rocks is an important parameter for safety analyses, as it is utilized to calculate the sorption database (K_d values) for the near-field (bentonite) and far-field field (i.e., Opalinus Clay) (Baeyens et al., 2014) of the deep geological radioactive waste repository. Besides other parameters, CEC and exchangeable cation occupancies play a critical role in the geochemical modelling of interstitial porewater compositions as demonstrated in Section 3.3 for the Opalinus Clay.

The 2:1 clay mineral content and CEC values illustrated in the Füchtbauer diagram of Fig. 6 show multiple trends as a function of lithology, indicating a relationship between mineralogical composition and CEC data. Specifically, the 2:1 clay mineral content and CEC values are elevated in the clay rich lithologies (i.e., claystones, argillaceous marl) and decrease towards clay poor lithologies (i.e., limestone and silt-/sandstone).

The fractional cation occupancies of the alkaline-earth metals remain consistently constant across all end-members, except for silt-/sandstone, which is only represented by two samples. Similarly, the fractional cation occupancies of the alkaline metals exhibit relatively constant values with slight variations observed for N_{K+NH4} and N_{Na}, which are lower in the limestone and silt-/sandstone units.

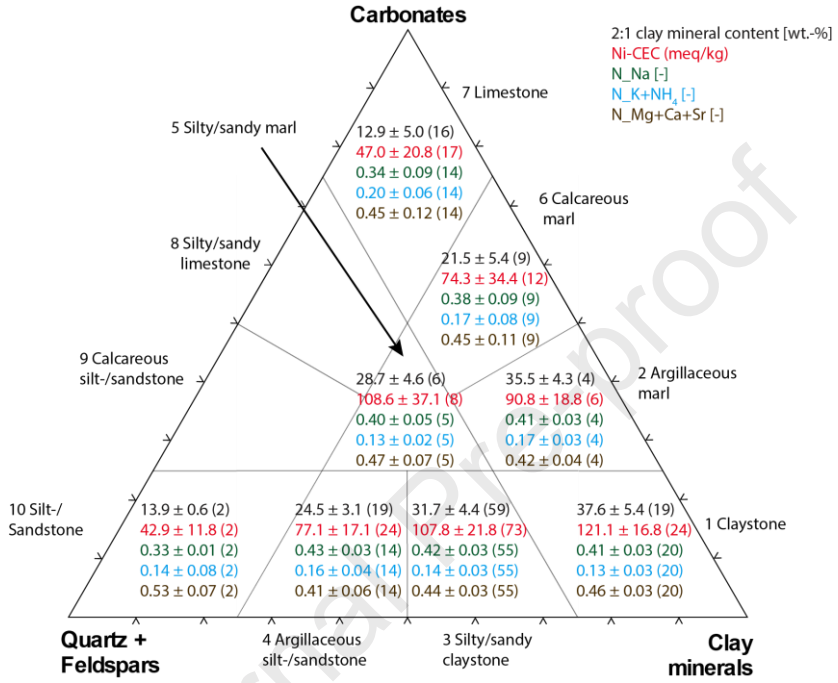

Fig. 6. Füchtbauer triangle (Füchtbauer, 1988) illustrating the values for 2:1 clay mineral content (illite + smectite + chlorite end-members), Ni-CEC, and fractional occupancy (average ± stdv, number of samples) for all samples (PSI and RWI) of this study. Axes of total carbonate (top), quartz + feldspars (bottom left) and total clay (bottom right) contents are in wt.% and the lithological types 1–10 according to Füchtbauer (1988) are indicated.

3.3. Porewater calculations for the Opalinus Clay

Based on the parameter values provided in this study and the experimental and modelling procedure described in previous studies (e.g., Bradbury and Baeyens (1998) and Gaucher et al. (2006)), a methodology can be employed to estimate simplified in-situ porewater compositions of argillaceous rocks. The knowledge is important for the long-term safety assessment of radionuclide (RN) transport as it *e.g.*, impacts RN mobility, barrier performances, corrosion and degradation, or redox conditions. Here, the focus is on Opalinus Clay because it is the most important formation for the safety assessment. In addition, we can compare the calculated

porewater compositions directly with the results from the SQ and AD experiments, which were determined on Opalinus Clay samples (Kiczka et al., 2023).

The mineralogical and physico-chemical data obtained for the Opalinus Clay across the three study areas are used in this study, and the averaged parameter values serve as the basis for the porewater calculations.

3.3.1. Summary of the mineralogical and physico-chemical parameters

Table 3 summarizes the data obtained from Opalinus Clay samples from the three study areas for 14 PSI and 4 RWI samples from ZNO, 21 PSI and 8 RWI samples from NL and 12 PSI and 4 RWI samples from JO. The experimental data for each rock sample is documented in the SI. A brief discussion on the selected parameters is given below.

Table 3: Summary of mineralogical and physico-chemical parameters for the Opalinus Clay from ZNO, NL and JO. The results represent average values (standard deviation) for the data obtained from all PSI and RWI samples.

	ZNO	**NL**	**JO**
	MAR1-1, TRU1-1	**STA2-1, STA3-1, BUL1-1**	**BOZ1-1, BOZ2-1**
Mineralogy [wt.%]			
Clay minerals	58.4 (8.0)	54.2 (10.4)	59.7 (9.4)
Calcite	8.5 (5.0)	9.2 (6.8)	7.5 (3.9)
Quartz	21.4 (4.0)	23.0 (6.8)	20.7 (6.1)
Siderite	2.5 (1.6)	3.6 (2.0)	3.9 (1.7)
Pyrite	1.0 (0.5)	0.8 (0.6)	0.6 (0.5)
Cation exchange capacity [meq/kg]			
Ni-CEC	106.9 (13.0)	104.0 (22.0)	114.6 (13.9)
ΣCATIONS	112.7 (18.3)	109.3 (25.1)	126.6 (20.2)
Extracted chloride [mmol/kg]			
Cl inventory	4.97 (0.65)	4.38 (0.50) 7.14 (0.74)	1.47 (0.35)
Water content relative to wet mass [wt.%]			
RWI data	4.84 (0.54)	4.40 (0.74)	5.26 (0.54)
Equivalent fractional occupancies (N_B values)			
N_{Na}	0.417 (0.019)	0.460 (0.036)	0.418 (0.022)
N_K	0.099 (0.021)	0.099 (0.034)	0.110 (0.027)
N_{NH4}	0.020 (0.001)	0.015 (0.003)	0.019 (0.002)
N_{Mg}	0.154 (0.013)	0.117 (0.015)	0.149 (0.016)
N_{Ca}	0.311 (0.024)	0.308 (0.027)	0.300 (0.012)
N_{Sr}	0.009 (0.001)	0.005 (0.001)	0.007 (0.002)

Mineralogical composition: The key minerals for modelling the in-situ porewater composition are clay minerals, carbonates, pyrite and quartz. Table 3 shows a high degree of consistency in the mineralogical composition of these minerals between the three study areas. The carbonate

minerals identified include calcite and siderite, while dolomite was identified in only one sample (MAR1-1 597.66). Although no anhydrite ($CaSO_4$) and celestite ($SrSO_4$) were detected in the mineralogical analysis of the rock samples, SO_4 was extracted from all samples. Aschwanden et al. (2023) observed that aqueous extractions resulted in much higher levels of SO_4 compared to concentrations measured in SQ or AD experiments. The geochemical modelling in this study assumes SO_4 to be fixed by celestite ($SrSO_4$). This is supported by the fact that porewaters obtained from SQ and AD are close to celestite equilibrium (Kiczka et al., 2023). Traces of celestite have also been identified in the Opalinus Clay under the scanning electronic microscope (SEM). The presence of siderite and pyrite can control the redox and Fe concentrations in the porewater, but this will not be examined in this study. Quartz was found ubiquitously and fixes the Si concentration in the porewater.

CEC: Table 3 provides the average Ni-CEC and ΣCATIONS cation exchange capacities of the Opalinus Clay samples. As previously discussed, ΣCATIONS values obtained from Cs-ex experiments are slightly higher than those obtained from Ni-ex experiments. However, the ΣCATIONS values reported in Table 3 are the average of both methods, which may be biased towards the larger sample batch of PSI. ΣCATIONS for JO are slightly higher than those for ZNO and NL. However, Ni-CECs as well as ΣCATIONS are consistent, and the averages fall within the calculated standard deviations for both methods. Since the exchangeable cation occupancies have been determined using the ΣCATION method, these data will be used in the modelling procedure (see Table 4).

Chloride inventory: Table 3 Indicates that the Cl inventory of the samples is not uniform and varies from 1.5 mmol/kg (BOZ1-1/BOZ2-1) to 7.1 mmol/kg (BUL1-1). The Cl inventory of cores within the JO and ZNO areas is consistent, whereas this is not the case for the area of NL. In the NL study area, the Cl inventories are similar for samples from STA2-1 and STA3-1 (4.4 mmol/kg), but higher in BUL1-1 (7.1 mmol/kg). Therefore, two distinct porewaters will be calculated for the NL area, considering the unique characteristics of the porewater in BUL1-1. It is noteworthy that the Opalinus Clay in BUL1-1 is more deeply buried than in the other boreholes.

Water content: Table 3 provides the average total water contents relative to wet mass in wt.% of the samples as determined by RWI. The values range between 4.4 to 5.3 wt.% and are, along with the accessible anion porosity, key parameters for the determination of the Cl concentrations in the in-situ porewater.

N_B values: The equivalent fractional occupancies exhibit another important parameter and constrains the porewater calculations. These cation occupancies act as a fingerprint of the exchange sites of the clay minerals with which the in-situ porewater is in thermodynamic equilibrium (Bradbury and Baeyens, 1998; Tournassat and Steefel, 2015). An interesting finding from these data is that the N_B values for each analysed exchangeable cation are very similar, with little variations, across the three study areas (Table 3). There are almost no differences between the N_B values for JO and ZNO whereas for NL there is a slightly higher Na loading compensated by a slightly lower Mg loading. The exchangeable NH_4 (1.5 to 2 %) obtained for the PSI samples and Sr (0.5 to 0.9 %) obtained either on PSI or RWI samples show the highest variability but are present at very low loadings.

3.3.2. Porewater model

The key parameters required for calculating a porewater composition and the model constraints are summarised in Table 4 and are briefly discussed below. The **temperature** is fixed at 25 °C. The **partial pressure of CO_2** is fixed to -2.2 log (bar), which is considered the most representative in-situ CO_2 partial pressure in Opalinus Clay porewaters, according to Wersin et al. (2022). The **CEC** values and exchangeable cation loadings (**N_B values**) are fixed according to the data given in Table 3. For the modelling, the N_B values together with ΣCATIONS have been converted in an equivalent scale in Table 4. The selectivity coefficients used in the geochemical modelling are taken from Pearson (1998) and are given in Table 4. The selectivity coefficient used for NH_4-Na exchange is identical to that of K-Na (De Preter, 1990).

Water content and Cl concentration: The total water contents (L/kg) in Table 4 are calculated from the values given in Table 3. Chloride accessible porosity factors (fa) for Opalinus Clay for ZNO and NL (fa = 0.47) and for JO (fa = 0.31) are taken from Zwahlen et al. (2023). These values are necessary to correct the total water content to the most representative volume in which Cl

(mol/kg) is dissolved. These corrections result in Cl concentrations varying from 0.09 M (JO) to 0.34 M (NL-BUL1-1). The stepwise procedure is illustrated in Table 4 for (i) ZNO (MAR1-1/TRU1-1), (ii) NL (STA2-1/STA3-1), (iii) NL (BUL1-1) and (iv) JO (BOZ1-1/BOZ2-1). The Cl concentrations are fixed in the four different porewaters calculated in section 3.3.3.

SO_4 concentrations: The SO_4 inventories of the Opalinus Clay samples exhibit variations ranging from 2 to 2.7 mmol/kg (see SI). If these inventories were to dissolve in the anion accessible porewater volumes, the resulting SO_4 concentrations would be significantly higher than those observed in SQ and AD experiments (Aschwanden et al., 2023). Additionally, these SO_4 concentrations would lead to precipitation of gypsum/celestite in the in situ porewater. For this reason, celestite was chosen to control SO_4 concentrations in the modelling. The cause of the SO_4 excess remains unclear, as discussed in Aschwanden et al. (2023).

Solid phases: The minerals calcite, celestite and quartz were taken to control CO_3, SO_4 and Si, respectively.

592 Table 4: Model for Opalinus Clay porewater compositions for JO, NL and ZNO regions.

Parameter	**Model constraint**	**Parameter value**			
		JO	**NL**		**ZNO**
		BOZ1-1, BOZ2-1	STA2-1, STA3-1	BUL1-1	MAR1, TRU1
T [°C]	Fixed	25			
log *p*-CO_2 [bar]	Fixed	-2.20			
pH		Defined by pCO_2			
CEC and exchangeable cations occupancies					
ΣCATIONS [meq/kg]	Fixed	126.6	109.3		112.7
Na^+ [meq/kg]	Fixed	52.7	50.1		46.4
K^+ [meq/kg]	Fixed	13.9	10.8		11.2
NH_4 [meq/kg]	Fixed	2.5	1.6		2.3
Mg^{2+} [meq/kg]	Fixed	18.8	12.7		17.3
Ca^{2+} [meq/kg]	Fixed	37.8	33.5		34.5
Sr^{2+} [meq/kg]	Fixed	0.9	0.6		1.0
Water content and Cl concentration					
H_2O content [L/kg]	Fixed	0.0526	0.0440		0.0484
Cl accessible porosity factor (fa) [-]	Fixed	0.31	0.47		0.47
Cl inventory [mol/kg]	Fixed	$1.47\ 10^{-3}$	$4.38\ 10^{-3}$	$7.14\ 10^{-3}$	$4.97\ 10^{-3}$
*Cl concentration [mol/L]	Fixed	0.090	0.21	0.34	0.22
TIC, SO_4 and Si concentrations					
TIC [mol/L]	Calcite saturation				
SO_4 [mol/L]	Celestite saturation				
Si [mol/L]	Quartz saturation				
Cation concentrations					
Na^+ [molL]	Charge balance				
K^+ [mol/L]	$^{K}_{Na}K_c = 16$				
NH_4 [mol/L]	$^{NH4}_{Na}K_c = 16$				
Mg^{2+} [mol/L]	$^{Mg}_{Na}K_c = 5$				
Ca^{2+} [mol/L]	$^{Ca}_{Na}K_c = 5$				
Sr^{2+} [mol/L]	$^{Sr}_{Na}K_c = 5$				

593 *Cl concentration $= \frac{\text{Cl inventory}}{\text{H}_2\text{O content} \cdot \text{fa}}$

594 *3.3.3. Porewater compositions for Opalinus Clay from ZNO, NL and JO*

595 Using the methodology proposed by Bradbury and Baeyens (1998) and the model constraints
596 summarized in Table 4, four different Opalinus Clay porewaters were calculated and the results
597 are summarized in Table 5. The modelling procedure followed is to hold the Cl concentrations
598 constant, while the concentrations of SO_4 and TIC are regulated by celestite and calcite/pCO_2,
599 respectively. The concentrations of Na, K, NH_4, Mg, Ca and Sr in the porewater are determined
600 by the fixed exchangeable cation loadings on the clay minerals via cation exchange reactions and
601 the corresponding selectivity coefficients. Ca and Sr are in addition controlled by mineral
602 equilibrium. The charge balance of the porewater is controlled by Na^+. Si concentration is fixed
603 by quartz saturation. The concentrations of Na, K, NH_4, Mg, Ca and Sr in the porewater are
604 determined by the exchangeable cation loadings on the clay minerals via exchange reactions and

605 the corresponding selectivity coefficients, except for Ca and Sr, which are in turn also controlled
606 by mineral equilibrium. Si concentration is fixed by quartz saturation. Table 5 indicates that the
607 trend observed for the four porewater compositions representing, BOZ1-1/BOZ2-1 (JO), MAR1-
608 1/TRU1-1 (ZNO), STA2-1/STA3-1 (NL) and BUL1-1 (NL), associated with a decreasing pH (7.3
609 to 6.9), an increasing ionic strength, *IS* (0.14 M to 0.40 M), increasing Na, K, Mg and Ca
610 concentrations, and decreasing TIC and SO_4 concentrations. In all porewater compositions,
611 dolomite and gypsum are undersaturated.

612 Table 5: Calculated porewater compositions for Opalinus Clay from the three study areas.

Region	**JO**	***NL**		**ZNO**
Borehole	**BOZ1-1/BOZ2-1**	**STA2-1/STA3-1**	**BUL1-1**	**MAR1-1/TRU1-1**
pCO_2 log (bar)	-2.2	-2.2	-2.2	-2.2
pH	7.28	7.08	6.94	7.03
I.S. (M)	0.14	0.26	0.40	0.27
Elements (M)				
Na	1.04×10^{-1}	1.82×10^{-1}	2.53×10^{-1}	1.67×10^{-1}
K	1.75×10^{-3}	2.50×10^{-3}	3.50×10^{-3}	2.60×10^{-3}
NH_4	3.00×10^{-4}	3.60×10^{-4}	4.80×10^{-4}	5.20×10^{-4}
Mg	4.10×10^{-3}	7.60×10^{-3}	1.44×10^{-2}	1.11×10^{-2}
Ca	8.01×10^{-3}	1.95×10^{-2}	3.63×10^{-2}	2.24×10^{-2}
Sr	1.90×10^{-4}	3.50×10^{-4}	6.70×10^{-4}	6.30×10^{-4}
Cl	9.00×10^{-2}	2.10×10^{-1}	3.40×10^{-1}	2.20×10^{-1}
^{VI}S (SO_4)	1.90×10^{-2}	1.40×10^{-2}	9.12×10^{-3}	8.20×10^{-3}
^{IV}C (TIC)	2.76×10^{-3}	2.00×10^{-3}	1.63×10^{-3}	1.87×10^{-3}
Si	1.80×10^{-4}	1.80×10^{-4}	1.80×10^{-4}	1.80×10^{-4}
SI of solid phases				
Calcite	0.0	0.0	0.0	0.0
Dolomite	-0.18	-0.29	-0.28	-0.18
Celestite	0.0	0.0	0.0	0.0
Gypsum	-0.44	-0.32	-0.35	-0.50
Quartz	0.0	0.0	0.0	0.0

613 *For NL two porewaters are calculated since Cl inventories were not the same in the different boreholes.

614 Figure 7 shows an overview of the molar concentrations of the cations (Na, K, Mg, Ca and Sr),
615 anions (Cl, SO_4 and TIC) and the pH of the porewaters obtained from (i) geochemical modelling,
616 (ii) SQ and (iii) AD experiments for the four different porewater compositions given in Table 5.
617 The SQ and AD data, obtained on Opalinus Clay samples from the same boreholes as the samples
618 used in this study, are taken from Kiczka et al. (2023).

619

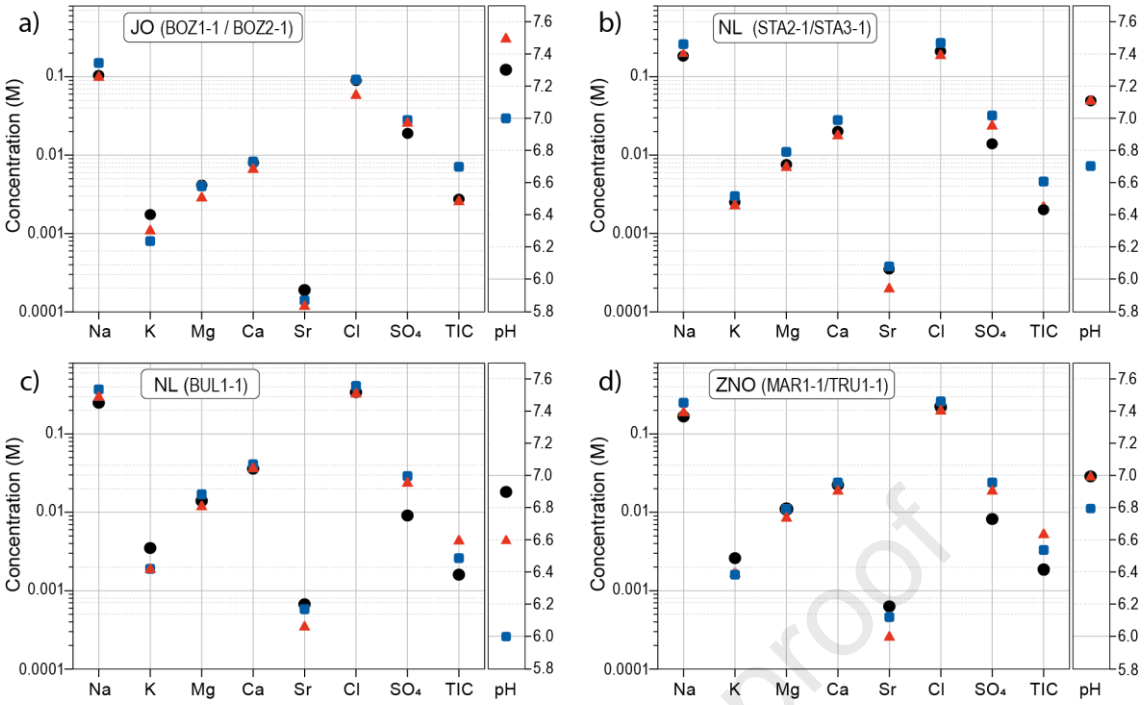

620

621 **Fig. 7.** Comparison of Opalinus Clay porewater compositions obtained from geochemical
622 modelling (●: Model), squeezing (▲: SQ) and advective displacement (■: AD) for (a) JO
623 (BOZ1-1/BOZ2-1), (b) NL (STA2-1/STA3-1), (c) NL (BUL1-1) and (d) ZNO (MAR1-1/TRU1-
624 1).

625 In the four different porewaters, Na dominates and is approximately two orders of magnitude
626 higher as K. The sequence of the alkaline-earth metal concentrations in all different porewaters
627 consistently follows Ca > Mg >> Sr. This very consistent behaviour originates from the similar
628 fractional cation occupancies of the Opalinus Clay samples as shown in Fig. 5a. The concentration
629 of the anions also follows a systematic sequence in all porewaters with Cl > SO_4 > TIC. The pH
630 varies from 6.6 to 7.5 for all porewaters with one exception of pH 6 obtained from the SQ
631 experiments for the BUL1-1 borehole (Fig. 7c).

632 A major outcome is the good agreement between all porewater compositions obtained by
633 modelling, SQ and AD. For Na, Mg, Ca and Cl the correspondence is very good. Slightly more
634 variability is observed for K, Sr, SO_4, TIC and pH. The modelled Sr and SO_4 concentrations are
635 systematically higher and lower, respectively, as the experimental data. This systematic difference
636 may be attributed to the assumption of celestite ($SrSO_4$) saturation in the modelling. The
637 somewhat greater variation in TIC/pH is likely due to the different approaches applied. In the
638 model calculations the pCO_2 was fixed at $10^{-2.2}$ bar and consequently the pH/TIC is impacted by

639 this assumption. In the SQ and AD experiments, the carbonate system is more likely influenced
640 by the experimental conditions.

641 In summary, the data in Fig. 7 demonstrates a noteworthy consistency among the three different
642 approaches used and hence provide reasonable estimates of the in-situ porewater composition of
643 the Opalinus Clay. Moreover, it is important to highlight that the modelling approach used for
644 calculating in-situ porewater can be extended to any of the lithological end-members shown in
645 Fig. 6, providing that details of the anion-accessible porosity are available. The study already
646 incorporates essential and relevant parameters such as mineralogical composition, water content,
647 Cl inventory, CEC, and cation occupancies, facilitating the applications of this approach to any
648 of the other lithological units.

649 **4. Summary and conclusions**

650 A mineralogical and physico-chemical characterisation has been carried out on large number
651 of core samples collected from seven different boreholes from the three study areas (JO, NL,
652 ZNO) within the Mesozoic cover of Northern Switzerland. The aim of this study was to obtain a
653 detailed understanding of sorption properties of the formations selected for a deep geological
654 repository for radioactive waste to determine implications for radionuclide mobility and thus
655 long-term safety and barrier performance assessments. Evaluating the potential transport
656 behaviour of radionuclides relies, among others, on the assessment of mineralogy, cation
657 exchange capacities and the occupancy of exchangeable cations. Furthermore, these geochemical
658 data enable the determination of the in-situ porewater composition of the rock formations, which
659 was focused on the Opalinus Clay due to its significance as host rock for the repository.

660 In this study, the CEC values were derived by four different and independent methods. The use
661 of a highly selective index cations (Cs^+ and Ni-en^{2+}) in concentrations high enough to saturate the
662 cation exchange sites of the rock samples allows to determine directly the Ni-CEC
663 and Cs-CEC by measuring the consumption of the index cation. The correlation between both
664 methods was found to be good. Cs-CEC values tended to be higher than Ni-CEC data due to the
665 higher K extraction yields obtained from Cs adsorption on illite. The data for the exchangeable
666 cation loadings for Na, K, NH_4, Mg, Ca and Sr of each rock sample were obtained from the Cs

667 and Ni-en extraction experiments (PSI and RWI samples, respectively), after correction with the
668 dissolved anions in the extraction solutions. The sum of the exchangeable cation occupancies
669 provided a third method for estimating the CEC, *i.e.*, Σ CATIONS of the rock samples. A fourth
670 method for estimating the CEC (Clay-CEC_{CALC}) was obtained from a theoretical calculation from
671 the detailed clay mineralogy, which included illite, smectite, kaolinite and chlorite content, and
672 the corresponding CEC values of the pure clay minerals.

673 The study found that clay-rich members, such as claystone and argillaceous marl, have high
674 CEC values, while clay mineral poor members, such as limestone and silt/sandstone, exhibit the
675 opposite. A Füchtbauer triangle was used to illustrate multiple trends for a wide range of
676 lithological rock types, indicating the relationship between clay mineral content and physico-
677 chemical data. On the other hand, the fractional cation occupancies remain constant in almost all
678 rock samples with clay contents ≥ 20 wt. %.

679 By combining the mineralogical and physico-chemical data obtained for the Opalinus Clay of
680 the three study areas, in-situ porewater compositions were geochemically modelled for each study
681 area. The results were in good agreement with the compositions obtained directly from SQ and
682 AD methods.

683 In essence, the integration of mineralogical and physico-chemical data provides a holistic
684 comprehension of the retardation behaviour of the geological formations targeted for deep
685 geological repositories. This forms the foundation for the development of models that can predict
686 the long-term retardation and migration of radionuclides through the geological. The findings of
687 this study are therefore significant in advancing the characterization and assessments of
688 performance of potential repository sites for the safe disposal of radioactive waste.

689 **Acknowledgements**

690 Astrid Schaible and Cyrill Lang carried out the experimental work. Sabrina Frick and Andreas
691 Laube performed the analytical measurements. Their contributions to this study are gratefully
692 acknowledged. The authors thank members of the RWI (University of Bern), in particular C.
693 Zwahlen, and members of Nagra, in particular D. Traber and J. Becker, for sample selection,
694 evaluation and auxiliary data support. The technical drawing office at Nagra is thanked for

finalizing the figures. Nagra (National Cooperative for the Disposal of Radioactive Waste, Wettingen, Switzerland) is also thanked for providing the samples and for financial support.

References

Allard, B., Karlsson, F., Tullborg, E.L., Larson, S., 1983. Ion exchange capacities and surface areas of some major components and common fracture filling materials of igneous rocks. SKB TR-83-64, Svensk Kärnbränslehantering AB.

Aschwanden, L., Wersin, P., Debure, M., Traber, D., 2023. Experimental study of sulphate in the Opalinus Clay porewater Applied Geochemistry.

Baeyens, B., Bradbury, M.H., 2004. Cation exchange capacity measurements on illite using the sodium and cesium isotope dilution technique: Effects of the index cation, electrolyte concentration and competition: Modeling. Clays Clay Miner. 52, 421-431.

Baeyens, B., Marques Fernandes, M., Bradbury, M.H., 2014. Comparison of Sorption Measurements on Argillaceous Rocks and Bentonite with Predictions Using the SGT-E2 Approach to Derive Sorption Data Bases. Nagra technical report NTB 12-05, Nagra, Wettingen, Switzerland.

Blanc, P., Legendre, O., Gaucher, E.C., 2007. Estimate of clay minerals amounts from XRD pattern modeling: The Arquant model. Physics and Chemistry of the Earth, Parts A/B/C 32, 135-144.

Bradbury, M.H., Baeyens, B., 1995. A Quantitative Mechanistic Description of Ni, Zn and Ca Sorption on Na- Montmorillonite. Part I: Physico-Chemical Characterisation and Titration Measurements. Nagra Technical Report NTB 95-04.

Bradbury, M.H., Baeyens, B., 1998. A physicochemical characterisation and geochemical modelling approach for determining porewater chemistries in argillaceous rocks. Geochimica et Cosmochimica Acta 62, 783-795.

Christidis, G.E., Chryssikos, G.D., Derkowski, A., Dohrmann, R., Eberl, D.D., Joussein, E., Kaufhold, S., 2023. Methods for Determination of the Layer Charge of Smectites: A Critical Assessment of Existing Approaches. Clays and Clay Minerals 71, 25-53.

Davies, C.W., 1962. Ion association. Butterworths, Washington.

De Preter, P., 1990. Radiocesium retention in the aquatic, terrestrial and urban environment: A quantitative and unifying analysis. PhD thesis, Katholieke Universiteit Leuven.

Füchtbauer, H., 1988. Sedimente und Sedimentgesteine, 4. Aufl. Schweizerbart, Stuttgart.

Gaines, G.L.J., Thomas, H.C., 1953. Adsorption studies on clay minerals. II. A formulation of the thermodynamics of exchange adsorption. Journal of Chemical Physics 21, 714.

Gaucher, É.C., Blanc, P., Bardot, F., Braibant, G., Buschaert, S., Crouzet, C., Gautier, A., Girard, J.-P., Jacquot, E., Lassin, A., Negrel, G., Tournassat, C., Vinsot, A., Altmann, S., 2006. Modelling the porewater chemistry of the Callovian–Oxfordian formation at a regional scale. Comptes Rendus Geoscience 338, 917-930.

Hadi, J., Wersin, P., Mazurek, M., Waber, H.N., Marques Fernandes, M., Baeyens, B., Honty, M., De Craen, M., Frederickx, L., Dohrmann, R., Fernandez, A.M., 2019. Intercomparison of CEC Method within the GD Project, in: 2017-06, M.T.T.R.T. (Ed.).

Kiczka, M., Wersin, P., Mazurek, M., Zwahlen, C., Jenni, A., Mäder, U., 2023. Porewater composition in clay rocks explored by advective displacement and squeezing experiments. Appl. Geochem. xx. Applied Geochemistry.

Mazurek, M., Aschwanden, L., 2020. Multi-scale Petrographic and Structural Characterisation of the Opalinus Clay. Arbeitsbericht NAB 19-44.

Mazurek, M., Gimmi, T., Zwahlen, C., Aschwanden, L., Gaucher, E., Kiczka, M., Rufer, D., Wersin, P., Marques Fernandes, M., Glaus, M.A., Van Loon, L., Traber, D., Schnellmann, M., Vietor, T., 2023. Swiss deep drilling campaign 2019–2022: Geological overview and rock properties with focus on porosity and pore geometry Applied Geochemistry.

Pawley, G.S., 1981. Unit-cell refinement from powder diffraction scans. Journal of Applied Crystallography 14, 357-361.

Pearson, F.J., 1998. Artificial Waters for Use in Laboratory and Field Experiments with Opalinus Clay: Status June 1998. TM 98-44-08 Paul Scherrer Institut

Peigneur, P., 1976 Stability and adsorption affinity of some transition metal-amine complexes in aluminosilicates. Ph.D Thesis, Univ. Leuven, Belgium.

Rietveld, H., 1969. A profile refinement method for nuclear and magnetic structures. Journal of Applied Crystallography 2, 65-71.

Thoenen, T., Hummel, W., Berner, U., Curti, E., 2014. The PSI/Nagra Chemical Thermochemical Database 12/07. PSI Bericht Nr. 14-04. Paul Scherrer Institut, Villigen.

Tournassat, C., Steefel, C.I., 2015. Ionic Transport in Nano-Porous Clays with Consideration of Electrostatic Effects. Reviews in Mineralogy and Geochemistry 80, 287-329.

Wersin, P., Gimmi, T., J., M., Mazurek, M., Zwahlen, C., Aschwanden, L., Gaucher, E., Traber, D., 2023. Profiles of Cl and Br in boreholes penetrating the Mesozoic sequence in northern Switzerland Applied Geochemistry.

Wersin, P., Mazurek, M., Gimmi, T., 2022. Porewater chemistry of Opalinus Clay revisited: Findings from 25 years of data collection at the Mont Terri Rock Laboratory. Applied Geochemistry 138, 105234.

Westall, J., Zachary, J.L., Morel, F., 1976. MINEQL, a computer program for the calculation of chemical equilibrium composition of aquous systems. Technical Note 18. Department of Civil Engeneer, Massachusetts Institute of Technology, Cambridge, Massachusetts.

Zwahlen, C., Gimmi, T., Jenni, A., Kiczka, M., Mazurek, M., Van Loon, L., Mäder, U., Traber, D., 2023. Chloride accessible porosity fractions across the Jurassic sedimentary rocks of northern Switzerland Applied Geochemistry.

Declaration of interests

☐ The authors declare that they have no known competing financial interests or personal relationships that could have appeared to influence the work reported in this paper.

☒ The authors declare the following financial interests/personal relationships which may be considered as potential competing interests:

Maria Marques Fernandes reports financial support was provided by Nagra. Paul Wersin, Martin Mazurek, Bart Baeyens reports financial support was provided by Nagra.